Research Article

Rapid Communications in Mass Spectrometry

Received: 22 February 2011 Revised: 7 August 2011 Accepted: 7 August 2011 Published online in Wiley Online Library

Rapid Commun. Mass Spectrom. **2011**, *25*, 3314–3322
(wileyonlinelibrary.com) DOI: 10.1002/rcm.5215

A novel hydrogen migration of dialkylphosphonic acid esters using electrospray ionization tandem mass spectrometry

Zhiping Zeng[1], Ping Luo[1], Yao Jiang[1], Yan Liu[1], Guo Tang[1], Pengxiang Xu[1] and Yufen Zhao[1,2]*

[1]Department of Chemistry and the Key Laboratory for Chemical Biology of Fujian Province, College of Chemistry and Chemical Engineering, Xiamen University, Xiamen 361005, P.R. China
[2]The Key Laboratory for Bioorganic Phosphorus Chemistry and Chemical Biology (Ministry of Education), Department of Chemistry, School of Sciences, Tsinghua University, Beijing 100084, P.R. China

In this paper, attention is focused on analysis of the fragmentation of α-hydroxy-β-amino phosphonate esters designed as inhibitors of protein kinase A. An interesting proton migration mechanism in the cleavage of the P-C bond is investigated by electrospray ionization tandem mass spectrometry. A possible rearrangement mechanism is proposed and verified by high-resolution mass spectra using isotope deuterium/hydrogen-exchange technology and additionally checked by detailed DFT calculation based on Gaussian software. The result clearly indicates that this mechanism proceeds by a five-membered ring concerted transition state with activation energy 11.3 kcal mol^{-1} for the compound 3f. The overall reaction is endothermic with an energy 13.2 kcal mol^{-1}. The effect of different substituents and different metal ions for rearrangement of these esters is studied by experiment and theory. It is concluded that this rearrangement process is energetically unfavorable and hence only occurs in the mass spectrometer.

Organophosphorus compounds containing a P–C bond were first isolated from living organisms in 1959.[1,2] Soon afterwards many kinds of related compounds were found in hundreds of aquatic and terrestrial animals and microorganisms.[3] α-Hydroxyphosphonate esters, considered as an important class of biologically active compounds, have attracted attention because of their antibacterial, antiviral, antibiotic, pesticidal, anticancer, and enzyme inhibitor properties.[4,5] However, the compounds under investigation here, α-hydroxy-β-aminophosphonate esters designed as inhibitors of protein kinase A, have not been reported previously. Hence a study of the fragmentation behavior of these compounds by electrospray ionization tandem mass spectrometry (ESI-MS/MS) is designed to deepen the understanding of their fragmentation structures.

Mass spectrometry is a very powerful tool and a unique physical method for structural determination in chemistry today. Electrospray ionization multistage tandem mass spectrometry (ESI-MS^n), coupled with high-performance liquid chromatography, has been widely developed in biological research, such as detection of non-covalent complexes,[6] the sequencing of proteins and polynucleotides,[7–9] pharmakinetics,[10] and drug metabolism.[11] In this present work, we synthesized a group of phosphonate esters and investigated their fragmentation behavior by electrospray ionization mass spectrometry combined with tandem mass spectrometry. A five-membered ring proton transfer mechanism was observed and checked by Fourier transform mass spectrometry (FT-MS) and subsequently this mechanism was elucidated in detail based on a theoretical study.

* *Correspondence to:* Y.-F. Zhao, Department of Chemistry and the Key Laboratory for Chemical Biology of Fujian Province, College of Chemistry and Chemical Engineering, Xiamen University, Xiamen 361005, P.R. China.
E-mail: yfzhao@xmu.edu.cn

EXPERIMENTAL

Mass spectrometric conditions

All the experiments were performed in the positive ion mode using a Bruker Esquire 3000plus ion trap mass spectrometer (Bruker Daltonic Inc., Billerica, MA, USA) equipped with an analytic electrospray ionization (ESI) source. Nitrogen was used as the drying gas at a flow rate of 4 L·min^{-1}. The nebulizer pressure was 8 psi and the electrospray capillary was typically held at 4 kV. The heated capillary temperature was 250 °C. Compounds, dissolved in methanol at a concentration of ca. 0.01 mg·mL^{-1}, were ionized by ESI and infused continuously into the ESI chamber at a flow rate of 4 μL·min^{-1} using a model 74900 syringe pump (Cole-Parmer Instrument Co., Vernon Hills, IL, USA). Generally, the scan range was from *m/z* 50 to 800. Five scans were averaged for each spectrum. All of the adducts, obtained from endogenous sources as their sodium salts, were selected using an isolation width of 1.0 to 1.5 mass-to-charge (*m/z*) units and analyzed by multistage tandem mass spectrometry through collision with helium to obtain the ESI-MS^n spectra. The fragmentation amplitude values ranged from 0.3 to 0.8 V and the fragmentation time was 40 ms.

Rapid Communications in Mass Spectrometry

The high-resolution tandem mass spectrum of deuterium-labeled compound **3c** was acquired on a Bruker APEX-Ultra Fourier transform ion cyclotron resonance (FT-ICR) mass spectrometer equipped with an analytic ESI source in the positive ion mode. Acquisition parameters were as follows: drying gas temperature, 180 °C; drying gas flow rate, 5.0 L min^{-1}; nebulizer gas flow rate, 1.0 L min^{-1}; ion accumulation time, 2.0 s. The following voltages were used: Capillary entrance voltage (4.3 kV), end plate (3.8 kV), skimmer 1 (36 V), and collision energy (13.5 V). The scan range was from *m/z* 100 to 700. The sample dissolved in CH_3OD was introduced into the source at a flow rate of 4 μL·min^{-1}. Ten scans were averaged for each spectrum.

For deuterium-labeling, compound **3c** (20 mg) was added to CH_3OD solvent(1 mL) and this solution was incubated with for 24 h at room temperature for exchange of active protons. An aliquot of the reaction mixture (10 μL) was diluted with CH_3OD (1 mL) and analyzed by ESI-FT-ICR-MS/MS. The ESI source was equilibrated before performing this experiment.

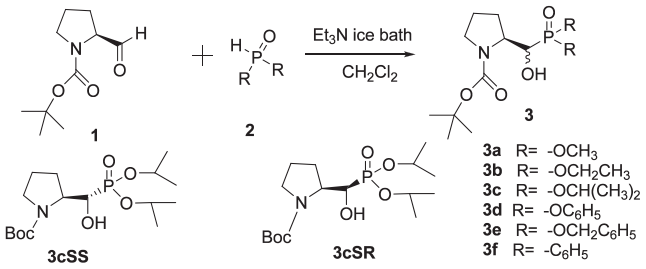

Scheme 1. Synthetic pathway for formation of compounds **3a–f**.

Theoretical calculations

Quantum chemical calculations were carried out on all the various species occurring in the rearrangement process in order to understand the atomic details of the main fragmentation reactions of the rearrangement ion. All calculations were performed with the GAUSSIAN 03 package.[12] The hybrid density functional method including Becke's three-parameter non-local-exchange functional[13] with the correlation functional of Lee-Yang-Parr[14] (B3LYP) was employed. The basis set used was the standard all-electron split-valence basis set 6-31 G* including the polarization d-function on non-hydrogen

Table 1. ESI-MS/MS of $[P + Metal]^+$ ions of compounds **3a–f** [*m/z*, relative abundance (%)]

		Product ions *m/z* (%)						
Compound (MW)	Precursor $[P + M]^+$	$[a + M]^+$ m-56	$[b + M]^+$ m-100	$[c + M]^+$ m-199	$[d + M]^+$ 122	$[e + M]^+$ 166	$[f + H]^+$ 200	$[f + Na]^+$ 222
3a	332(3)	276(28)	232(100)	133(7)	122(23)	166(<1)	200(<1)	222(3)
Na	276(12)		232(100)	133(3)	122(10)	166(<1)	200(<1)	222(0)
	232(20)			133(25)	122(100)	166(0)	200(3)	222(0)
3b	360(18)	304(2)	260(100)	161(7)	122(12)	166(1)	200(0)	222(2)
Na	304(2)		260(100)	161(5)	122(13)	166(0)	200(0)	222(0)
	260(28)			161(60)	122(100)	166(0)	200(0)	222(0)
3cSR	388(1)	332(1)	288(100)	189(6)	122(4)	166(<1)	200(0)	222(1)
Na	332(40)		288(100)	189(<1)	122(<1)	166(0)	200(1)	222(0)
	288(74)			189(30)	122(21)	166(0)	200(0)	222(0)
3cSS	388(22)	332(17)	288(100)	189(2)	122(2)	166(<1)	200(0)	222(<1)
Na	332(45)		288(100)	189(<1)	122(<1)	166(0)	200(2)	222(0)
	288(84)			189(21)	122(25)	166(0)	200(0)	222(0)
3d	456(11)	400(100)	356(60)	257(28)	122(0)	166(<1)	200(0)	222(3)
Na	400(13)		356(100)	257(41)	122(5)	166(<1)	200(0)	222(0)
	356(76)			257(100))	122(11)	166(0)	200(0)	222(0)
3e	484(1)	428(15)	384(100)	285(45)	122(0)	166(1)	200(0)	222(2)
Na	428(52)		384(100)	285(13)	122(0)	166(0)	200(0)	222(0)
	384(13)			285(100)	122(2)	166(0)	200(0)	222(0)
3f[a]	402(12)	346(5)	302(100)	203(3)	100(0)	144(0)	178(0)	199(0)
H	302(8)			203(100)	100(49)	144(0)	178(0)	199(0)
3f[b]	408(6)	352(100)	308(96)	209(0)	106(0)	150(10)	184(0)	206(21)
Li	352(14)		308(100)	209(2)	106(4)	150(0)	184(0)	206(0)
	308(21)			209(2)	106(100)	150(0)	184(0)	206(0)
3f	424(20)		324(26)	225(0)	122(4)	166(17)	200(0)	222(100)
Na	324(15)			225(5)	122(100)	166(0)	200(0)	222(0)
	222(14)				122(13)	166(100)		
	166(42)				122(100)			
3f[c]	440(2)	384(0)	340(4)	241(1)	138(1)	182(2)	216(0)	238(100)
K	340(100)			241(43)	138(98)	182(0)	216(0)	238(0)

[a]ESI-MS/MS of the $[P + H]^+$ ions of compound **3f**.
[b]ESI-MS/MS of $[P + Li]^+$ ions of compound **3f**.
[c]ESI-MS/MS of $[P + K]^+$ ions of compound **3f**.

atoms.[15,16] We calculated the geometries and vibrational frequencies belonging to each reactant, product, transition state, and intermediate without any constraint. We confirmed that all the reactants and intermediates have no imaginary frequencies and each transition state had only one imaginary frequency. Reported energies are ZPE (zero-point energy)-corrected, unless otherwise specified.

Preparation of samples

Compounds **3a–f** were synthesized (see Scheme 1) according to methods described in the literature.[17] General procedures are shown as follows.

Compound **1** (1.0 mmol yellow oil), as the reactant, was injected into in a 5 mL flask containing 2 mL dichloromethane, and then compound **2** (1.2 mmol liquid) and triethylamine (0.4 mL) were added dropwise to the resulting solution. The reaction was monitored by thin-layer chromatography (TLC) until the reactant disappeared. The solvent was then removed under reduced pressure to obtain a slurry, purified by silica gel column chromatography (petroleum ether/ethyl acetate 1:1) to give products **3a–f** as colorless amorphous solids or liquids in yields of 83–90%. Each pair of the compounds **3a–f** was epimeric because the chirality of the connecting carbon of the hydroxyl group was induced by the L-proline. All of the structures were characterized by ^{31}P NMR, ^{1}H NMR, and ^{13}C NMR and elemental analysis.

The two diastereoisomers of compound **3c** were first purified by flash column chromatography and then re-chromatographed to separate them into pure diastereoisomers identified as **3cSS** and **3cSR**. The absolute configuration of compound **3cSR** was determined by X-ray diffraction analysis. Analytical data for these two compounds are as follow: **3cSS**: colorless oil, ^{1}H NMR (400 MHz, $CDCl_3$) δ 5.40 (s, 1H, OH), 4.88–4.71 (m, 2H, $CH(CH_3)_2$), 4.30–4.20 (m, 1H, CH(OH)), 3.71–3.63 (m, 1H, NCHC(OH)), 3.41–3.37 (m, 1H, NCHH), 3.37–3.30 (m, 1H, NCHH), 2.28–2.20 (m, 1H, NCHCHH), 2.05–1.95 (m, 1H, NCHCHH), 1.93–1.81 (m, 2H, NCH_2CH_2), 1.47 (s, 9H, $C(CH_3)_3$), 1.36 (dd, J = 6.2, 1.8 Hz, 12H, $CH(CH_3)_2$).^{13} C NMR (101 MHz, $CDCl_3$) δ 158.4 (C = O), 80.9 ($OC(CH_3)_3$), 73.1 (d, J = 160.9 Hz, 1 C, CH(OH)), 71.5 (d, J = 7.7 Hz, 1 C, $OCH(CH_3)_2$), 71.0 (d, J = 7.1 Hz, 1 C, $OCH(CH_3)_2$), 59.2(d, J = 6.8 Hz, 1 C, NCH), 47.1 (NCH_2), 29.7 ($NCHCH_2$), 28.4(s, 3 C,$C(CH_3)_3$), 24.2 (d, J = 3.4 Hz, 1 C, NCH_2CH_2), 24.05 (d, J = 3.7 Hz, 2 C, $CH(CH_3)_2$), 24.00(d, J = 4.0 Hz, 2 C, $CH(CH_3)_2$).^{31}P NMR (162 MHz, $CDCl_3$) δ 19.86. **3cSR**: white solid, ^{1}H NMR (400 MHz, $CDCl_3$) δ 4.87 (s, 0.7H, OH), 4.80–4.71 (m, 2H, $CH(CH_3)_2$), 4.35–4.09 (m, 2H, CH(OH) and NCHC(OH)), 3.59–3.48 (m, 1H, NCHH), 3.32 (dt, J = 10.6, 7.2 Hz, 1H, NCHH), 2.92 (s, 0.3H, OH), 2.36–2.20 (m, 1H, NCHCHH), 2.10–1.93 (m, 2H, NCHCHH and NCH_2CH_2), 1.76–1.66 (m, 1H, NCH_2CH_2), 1.48 (s, 9H, $C(CH_3)_3$), 1.34 (d, J = 6.1 Hz, 12H, $CH(CH_3)_2$).^{13} C NMR (126 MHz, $CDCl_3$) δ 156.4 (C = O), 80.0 ($OC(CH_3)_3$), 70.9 (d, J = 5.1 Hz, 2 C, $OCH(CH_3)_2$), 70.8 (d, J = 156.1 Hz, 1 C, CH(OH)), 60.2 (NCH), 47.8(NCH_2), 28.6 (s, 3 C, $C(CH_3)_3$), 27.5 ($NCHCH_2$), 24.2 (d, J = 3.2 Hz, 1 C, NCH_2CH_2), 24.07 (d, J = 4.1 Hz, 2 C, $CH(CH_3)_2$), 23.99 (d, J = 5.3 Hz, 2 C, $CH(CH_3)_2$).^{31}P NMR (162 MHz, $CDCl_3$) δ 20.82. ESI-HRMS calcd for $[C_{16}H_{32}NPO_6 + Na]^+$: 388.1859; found: 388.1852.

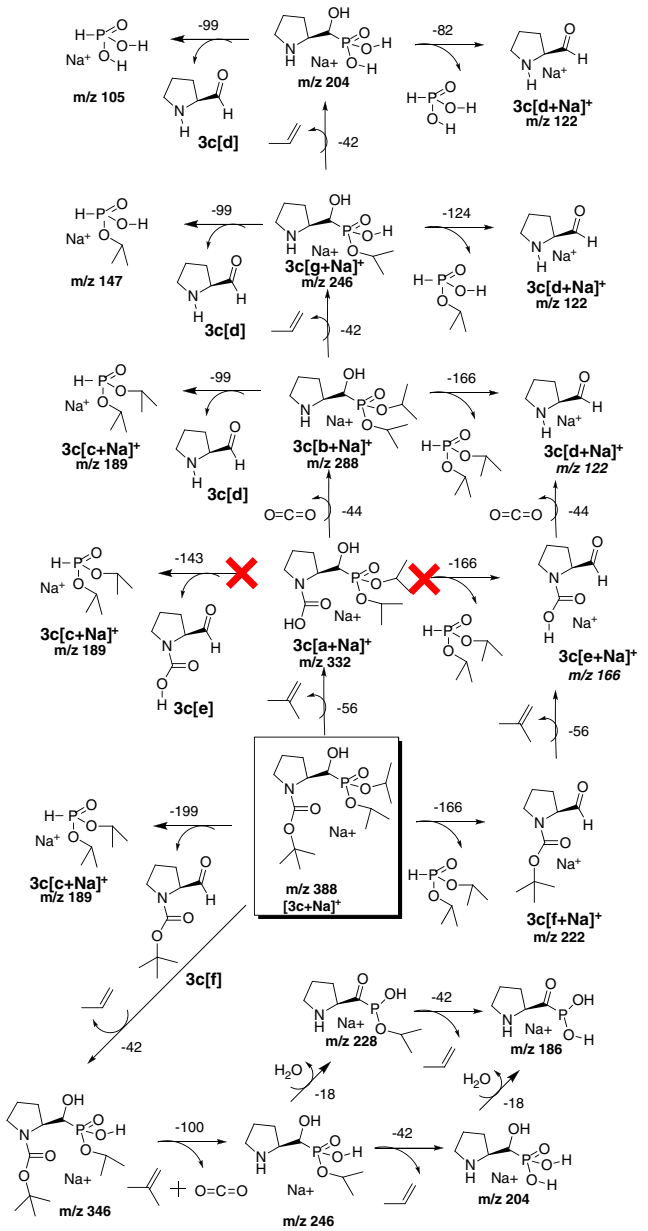

Scheme 2. Possible fragmentations of sodiated phosphonate cation from **3c**.

RESULTS AND DISCUSSION

ESI-MS fragmentation of 3a–f

We found that the analysis of compounds **3a–f**, (*S*)-*tert*-butyl-2-((*S* or *R*)-(dialkyoxyphosphoryl)(hydroxy)methyl)pyrrolidine-1-carboxylate, by ESI-MS only afforded the corresponding sodium ions $[P + Na]^+$. ESI-MS^n spectra of compounds **3a–f** in positive mode were studied in detail and the data are shown in Table 1. In addition, mass fragmentation of compound **3c** for a pair of diastereomers, labeled **3cSR** and **3cSS**, has been studied and there is no significant difference in their spectra (also see Supplementary Tables S2 and S3, Supporting Information). Thus, the fragmentation study of our samples **3a–f** with a mixture diastereomers is valid. Meanwhile, adduct ions of different cations of compound **3f** (H^+, Li^+, Na^+, K^+) were studied

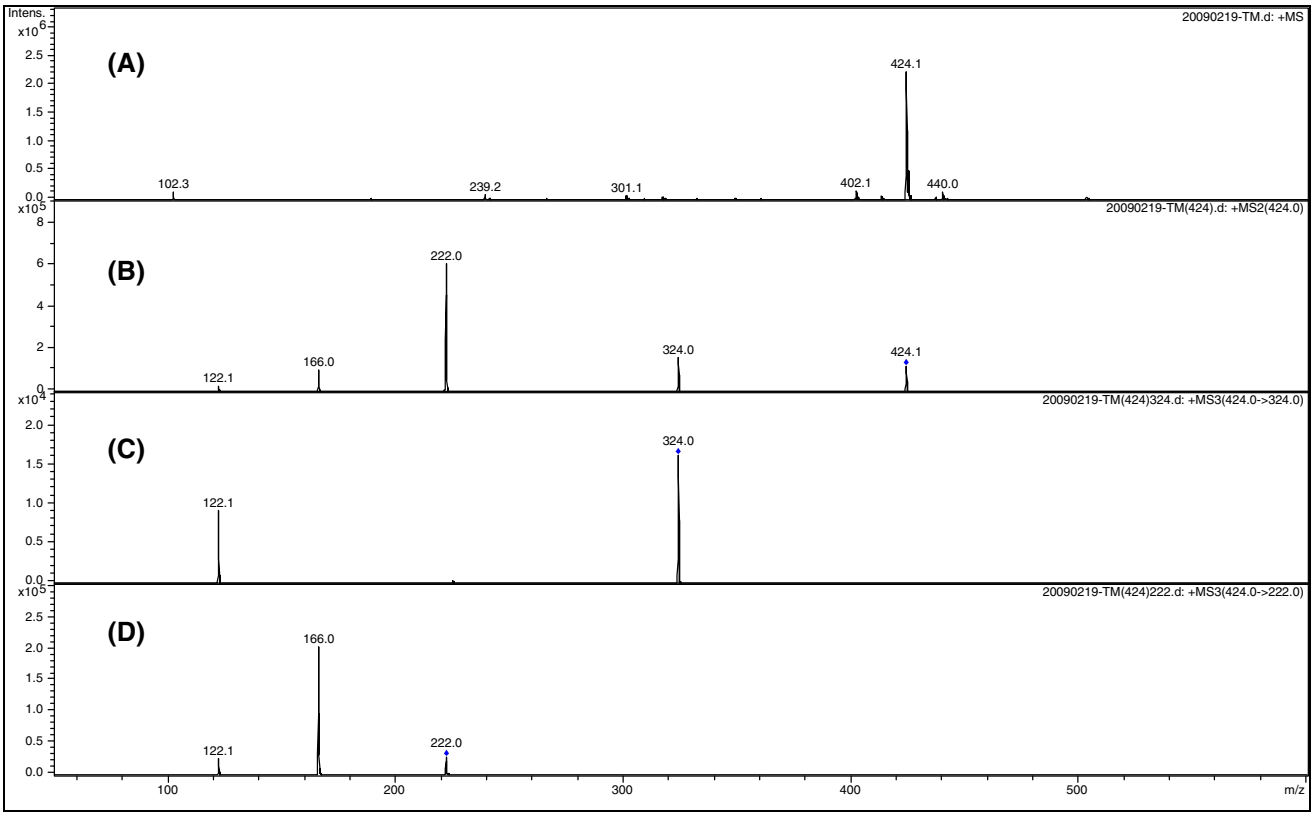

Figure 1. MS^n spectra from solidated **3f**: (A) MS of [**3f** + Na]$^+$; (B) MS^2 of [**3f** + Na]$^+$ at *m/z* 424; (C) MS^3 of the ion at *m/z* 324; and (D) MS^3 of the ion at *m/z* 222.

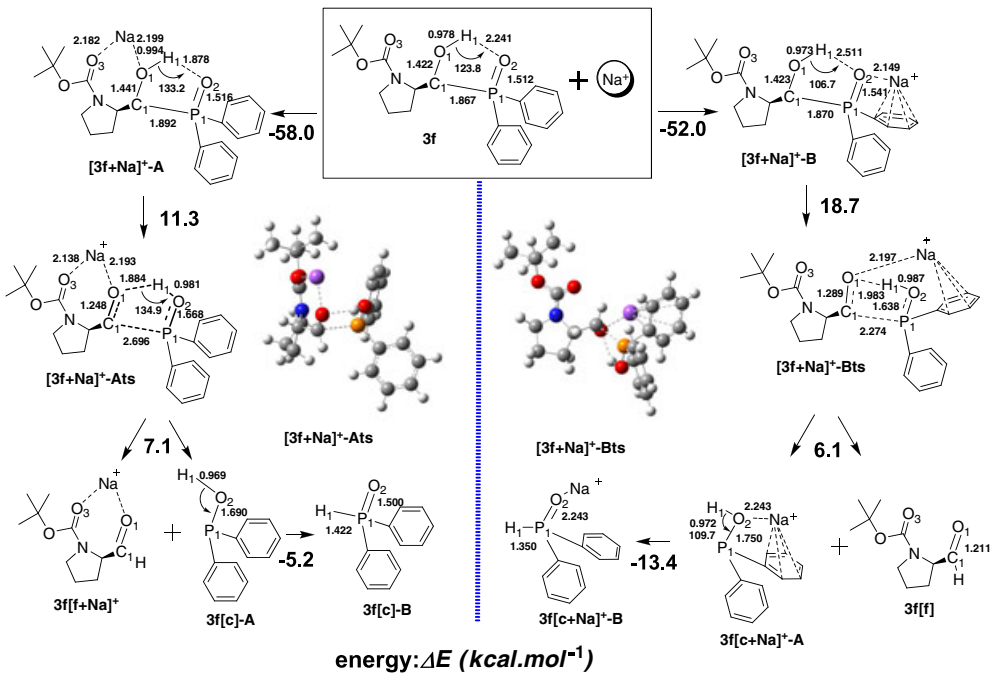

Scheme 3. Rearrangement mechanism and energy changes (kcal mol^{-1}) among reactants, transition states, and products of solidated **3f**.

in depth and the results used to investigate the mechanism of this metal-assisted fragmentation cleavage.

Comparison among the structures of compounds **3a–f**, which only differ in the alkyl or alkoxyl group of the phosphonates, reveals that the fragmentation patterns are correlated with the types of substituents of the phosphonates. Given that those compounds display similar patterns of fragmentation, the following discussion will focus on compound **3c** as an example. ESI-MS^n of the sodium ion adducts [**3c** + Na]$^+$ from **3c** affords product ions **3c**[a + Na]$^+$, **3c**[b + Na]$^+$, **3c**[c + Na]$^+$, **3c**[d + Na]$^+$, **3c**[e + Na]$^+$ and **3c**[f + Na]$^+$ (see Scheme 2). The signal at *m/z* 288 corresponding to the product ion **3c** [b + Na]$^+$, [P + Na-100]$^+$, is observed as the base peak. The fragment ion **3c**[a + Na]$^+$, product *m/z* 332, is produced by loss of 2-methylprop-1-ene (56 Da) from the *tert*-butoxycarbonyl group through cleavage of a carbon–oxygen bond, and this is a common fragmentation pathway for all the compounds.[18,19] The three hydrogen atoms of the methyl group all locate in the β-position carbon of the *tert*-butoxycarbonyl protecting group, one of which likely migrates from the methyl group to the oxygen of the carbonyl group. According to the McLafferty rearrangement, α,β-elimination occurs subsequently by cleavage of the quaternary carbon–oxygen bond in the *tert*-butoxycarbonyl protecting group. One neutral molecule, 2-methylprop-1-ene (56 Da), is released from the precursor ion [**3c** + Na]$^+$ and then product ion **3c**[a + Na]$^+$ is produced finally. Next carbon dioxide (44 Da) is lost from the fragment ion **3c** [a + Na]$^+$ to give ion **3c**[b + Na]$^+$ at *m/z* 288.[20] Similarly, product ions **3c**[d + Na]$^+$ and **3c**[e + Na]$^+$ were generated by loss of a molecule of 2-methylprop-1-ene (56 Da) or carbon dioxide (44 Da) from the precursor ion **3c**[f + Na]$^+$ as for the precursor ion [**3c** + Na]$^+$. In addition, ion [d + Na]$^+$ is derived from ion [e + Na]$^+$ as shown for the case of **3f** (see Table 1**)**. These three types of product ion were found in all the MS/MS spectra of the sodium ion adduct precursors obtained from the series of compounds (**3a–f**).

The P–C bonds of the precursor ion [**3c** + Na]$^+$ and its product ion **3c**[b + Na]$^+$ are fragmented by collision-induced dissociation (CID) to give ions **3c**[c + Na]$^+$, **3c**[d + Na]$^+$ and **3c** [f + Na]$^+$. Nevertheless, product ion **3c**[a + Na]$^+$ does not show the same cleavage pattern as for ions [**3c** + Na]$^+$ and **3c**[b + Na]$^+$ because this ion is so unstable that loss of carbon dioxide (44 Da) takes priority to give ion **3c**[b + Na]$^+$ (see Scheme 2). The product ion **3c**[c + Na]$^+$ at *m/z* 189 is the sodium ion of the phosphonate diisopropyl ester, formed by loss of (*S*)-*tert*-butyl 2-formylpyrrolidine-1-carboxylate (199 Da) from the precursor ion [**3c** + Na]$^+$. Also, ion **3c**[b + Na]$^+$ leads to ion **3c**[c + Na]$^+$ in a similar pathway by loss of (*S*)-pyrrolidine-2-carbaldehyde (99 Da). In addition, product ion **3c**[f + Na]$^+$ at *m/z* 222 (only observed in the ESI-MS^1) was detected as the sodium adduct of (*S*)-*tert*-butyl 2-formylpyrrolidine-1-carboxylate (199 Da). It is noteworthy that the intensity of product ions **3c**[f + Na]$^+$ in the MS spectra are extremely weak apart from compound **3f** (see Fig. 1**)**, where MS^2 of [**3f** + Na]$^+$ at *m/z* 424 shows product ion **3f**[f + Na]$^+$ is the base peak. By comparison with the other [f + Na]$^+$ fragmentations, it is found that the phenyl group of [**3f** + Na]$^+$ binds directly to phosphorus with the help of the P_1–C_{phenyl} bond which is more stable than the P_1–$C_1(O_1H_1)$ bond (see Scheme 3) and thus the latter ion takes priority in cleavage, producing an abundant ion **3f**[f + Na]$^+$ at *m/z* 222. For the compounds **3a–e**, the alkoxy group binds to phosphorus via the C_{alkyl}–$O(P_1 = O_2)$ bond, that is much more reactive than the P_1–$C_1(O_1H_1)$ bond so that an alkyl group is firstly removed from the alkoxy group by the cleavage of the P_1O–C_{alkyl} bond on collision (see Scheme 3). On the other hand, the alkoxy group exhibits some electronic and stereo effects in inhibiting the intensity of ion [f + Na]$^+$ (*m/z* 222) through inter- or intramolecular interaction.

Distinctive fragmentation ions are produced in the MS of the **3c** species (see Scheme 2), because of the easier loss of an isopropyl group by β-elimination from the precursor ion.[21–24] All the product ions from **3c** lose one or two 2-methylprop-1-ene species (42 Da), giving ions at *m/z* 346, 246, and 204. The β-position of the isopropoxyl group of the phosphonate has six hydrogen atoms, so this has a great probability to migrate one hydrogen to the bridging oxygen and give out one or two neutrals. Though ion [**3b** + Na]$^+$ has two ethoxyl groups, it does not show the same β-elimination mechanism, as no ethylene loss is observed in the MS^2 of [**3b** + Na]$^+$ to give *m/z* 360. In addition, water (18 Da) can be eliminated from all of these ions (*m/z* 246 and 204). It is possible that a three-coordinated phosphorus structure (see Scheme 2) is formed

Table 2. FTICR-ESI-MS of sodium ion adducts of **3cSR** and its product ions

Items	Fragmentation (*m/z*)	Exp.	Exact by calc.	Formula
[**3cSR** + Na]$^+$	388	388.1852(25)	388.1859	$C_{16}H_{32}NPO_6Na$
[**3cSR** + Na]$^{+*a}$	389	389.1918(33)	389.1922	$C_{16}H_{31}DNPO_6Na$
3cSR[a + Na]$^{+b}$	332	332.1228(4)	332.1227	$C_{12}H_{24}NPO_6Na$
3cSR[a + Na]$^{+*}$	333	333.1290(5)	333.1290	$C_{12}H_{23}DNPO_6Na$
3cSR[b + Na]$^+$	288	288.1330(100)	288.1329	$C_{11}H_{24}NPO_4Na$
3cSR[b + Na]$^{+*}$	289	289.1389(100)	289.1392	$C_{11}H_{23}DNPO_4Na$
3cSR[c + Na]$^+$	189	189.0659(4)	189.0651	$C_6H_{15}PO_3Na$
3cSR[c + Na]$^{+*c}$	189	189.0647(3)	189.0651	$C_6H_{15}PO_3Na$
	190	190.0710(3)	190.0713	$C_6H_{14}DPO_3Na$
3cSR[g + Na]$^+$	246	246.0867(21)	246.0860	$C_8H_{18}NPO_4Na$
3cSR[g + Na]$^{+*}$	247	247.0925(21)	247.0922	$C_8H_{17}DNPO_4Na$

a*: Asterisk marks mean deuterium experiments of [**3cSR** + Na]$^+$.
[b]**3cSR**[a + Na]$^+$ means the fragment ion a of [**3cSR** + Na]$^+$ in Table 1, similar to other items in column 1 of this table.
[c]**3cSR**[c + Na]$^{+*}$ contained two ions *m/z* 189 and 190 compared to **3cSR**[c + Na]$^+$.

to stabilize the adduct ions (*m/z* 228 and 186). It is intriguing that the precursor ion (*m/z* 346) does not lose water in this fragmentation, though two hydroxyl groups are adjacent at the α- and β-positions of these species. The ion at *m/z* 246, formed by loss of a monoalkyl phosphonate, is observed which implies the cleavage of the P–C bond. This phenomenon was also observed for the ion at *m/z* 204, likely because these phosphonic acids share a common cleavage mechanism.

Finally, it is noteworthy that formation of product ions $[c + M]^+$ (*m/z* 147 and 105) and $[f + M]^+$, $[d + M]^+$, and $[e + M]^+$ (see Table 1, containing $[f + H]^+$ and $[f + M]^+$) cannot be directly explained by a simple cleavage, because a novel proton migration occurs in this process.

Evidence for and mechanism of hydrogen migration

In order to validate the mechanism of formation of product ions $[c + M]^+$ and $[f + M]^+$, high-resolution ESI-MS/MS was performed for the sodium ion adducts of **3cSR** and its product ions (see Table 2). Secondly, spectra following deuterium exchange of compound **3cSR** were recorded by FT-ESI-MS (see Table 2, data with asterisks). The hydroxyl group of compound **3cSR** was deuterated fully, and its product ions **3cSR**$[a + Na]^{+}$* and **3cSR**$[b + Na]^{+}$*, both containing this hydroxyl group, showed an increase of 1 amu. It is notable that product ions **3cSR**$[c + Na]^{+}$* (190 Da), the sodium ion adduct of diisopropyl phosphonate from the precursor on $[\mathbf{3cSR} + Na]^{+}$*, appeared to be incompletely

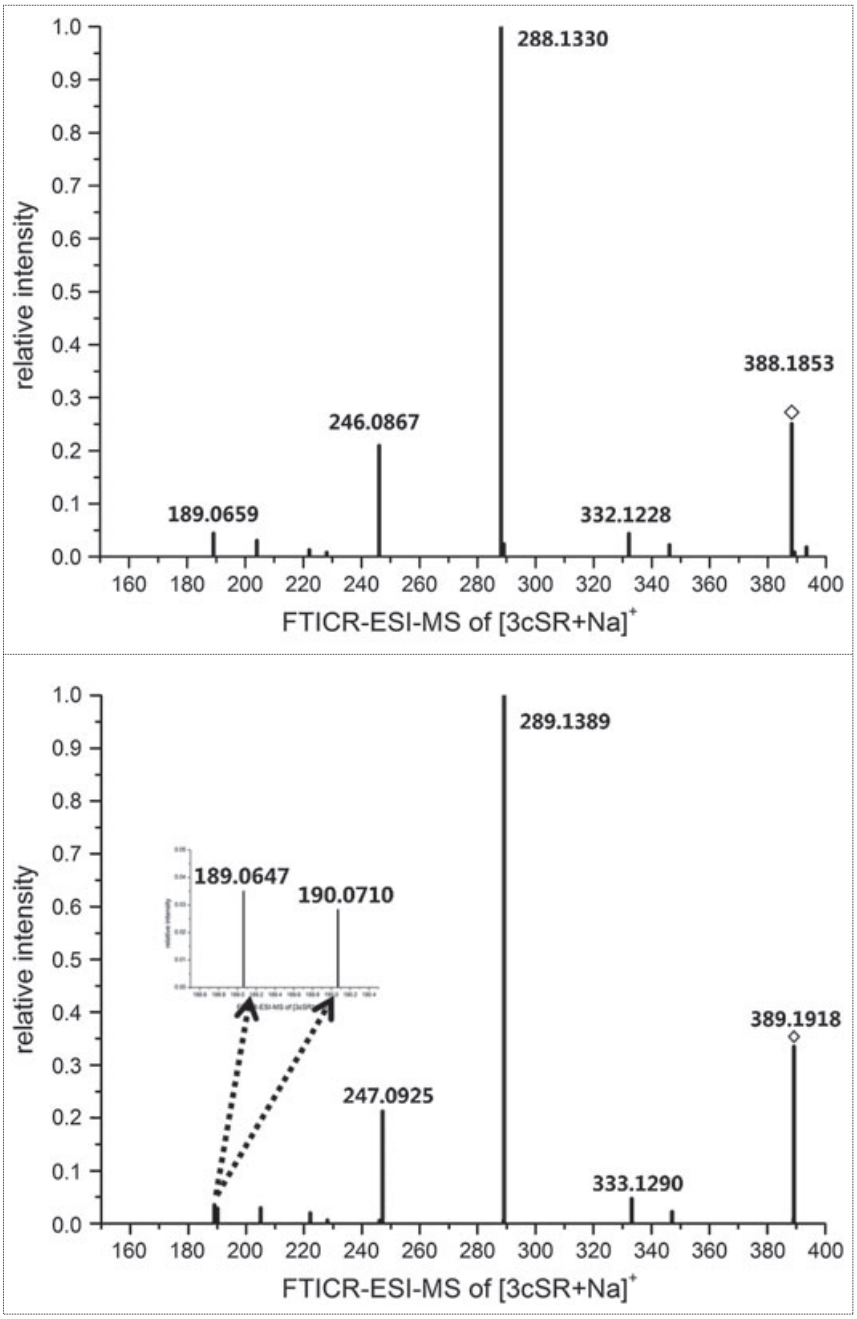

Figure 2. FTICR-ESI-MS/MS^2 of $[\mathbf{3cSR} + Na]^+$ (388.18528) and $[\mathbf{3cSR} + Na]^{+}$*.

deuterated. It could be that a deuterium atom from the hydroxyl group migrates to the phosphoryl group and the product ion **3cSR**[c + Na]$^{+*}$ is formed, exchanging with the active proton of product ion **3cSR**[f + Na]$^+$, and so partially converts into product ion **3cSR**[c + Na]$^+$ (189 Da). The ratio of these two ions was observed to be close to 1:1 (see Fig. 2). This explained the process in such a reaction, deuterium exchange in mass spectrometry to achieve a balance rapidly. In our further theoretical study, this effect also was taken into account to elucidate the migration mechanism (see Scheme 4).

It is worth noting that the spectrum of [**3f** + Na]$^+$ is different from the other species. It produced a more intense **3f**[f + Na]$^+$ ion and less intense **3f**[c + Na]$^+$ ion. In order to validate the mechanism of formation of these product ions, a five-membered ring proton transfer mechanism is proposed based on the experimental data (see Scheme 3). In addition, a theoretical calculation has been carried out using the density functional theory (DFT) method. According to the calculation results, the proton transfer mechanism can adopt a concerted pathway, involving two five-membered ring transition states [**3f** + Na]$^+$–**Ats** and [**3f** + Na]$^+$–**Bts**, which depend on the binding position of the sodium ion. The activation energy of the transition state for pathway **A** is 11.3 kcal mol^{-1}, which is 7.4 kcal mol^{-1} lower than transition state of pathway **B** (18.7 kcal mol^{-1}). Moreover, the energy of the sodium-binding process of pathway **A** is exothermic by about −58.0 kcal mol^{-1}, that is 6.0 kcal mol^{-1} more than for pathway **B**. For these two reasons, pathway **A** is energetically more favorable to promote the proton transfer process and produce the fragment ion **3f**[f + Na]$^+$, which is in accord with the experimental data. Overall, both reaction pathways are endothermic with predicted reaction energies of 7.1 kcal mol^{-1} and 6.1 kcal mol^{-1} (see Scheme 3). To determine the favored transition state for [**3f** + Na]$^+$–**Ats**, the deuterium kinetic isotope effect of [**3cSR** + Na]$^+$ was taken into consideration in the theoretical modeling based on results from the D/H exchange experiment. The activation energy of the rate-limiting step for the dissociation of [**3cSR** + Na]$^{+*}$ (22.4 kcal mol^{-1}) is 0.1 kcal mol^{-1} higher than for [**3cSR** + Na]$^+$ (22.3 kcal mol^{-1}), suggesting that deuteration does not change the reaction pathway (see Scheme 4 and Supplementary Fig. 13, see Supporting Information).

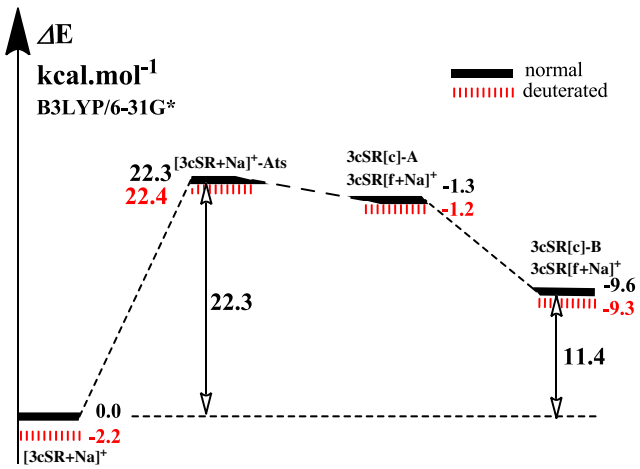

Scheme 4. Computed (B3LYP/6-31G*) energy changes for the transition state and products in the fragmentation of [**3cSR** + Na]$^+$ and its corresponding deuterated products.

In this concerted mechanism of pathway **A**, one intermolecular hydrogen bond of [**3f** + Na]$^+$–**A** is formed between the alpha-hydroxyl group and the phosphoryl oxygen. The bond length and angle are 1.878 Å and 133.2° (see Scheme 3), which means that the hydrogen bond is so strong that it plays a predominant role in stabilizing this structure. Next, lengthening of the P_1–C_1 bond is observed in the transition state of [**3f** + Na]$^+$–**Ats** with its bond length changing from 1.892 Å to 2.700 Å. At the same time, hydrogen migrates from the hydroxyl group to the phosphoryl group, resulting in the formation of a tri-coordinate diisopropyl phosphonate intermediate (**3f[c]–A**) accompanied by oxidation of the hydroxyl group to a carbonyl group. This process is endothermic, with some 7.1 kcal mol^{-1} energy absorbed in this step (see Scheme 4). Finally, this tri-coordinate diisopropyl phosphonate intermediate is so unstable that it rapidly converts into a tetra-coordinate phosphonate (**3f[c]–B**), releasing energy of about 5.2 kcal mol^{-1}.

Based on this mechanistic analysis, we investigated the relationship of the nature of the phosphonate alkyl group to the intensity of the rearrangement ion (see the [f + M]$^+$ column in Table 3). Experimentally, we found that the greater the steric bulk of the alkyl group, the greater the intensity of the rearrangement ion. A DFT calculation based upon Gaussian was introduced to optimize the transition state for

Table 3. Computed transition state structures and activation barriers in the hydrogen migration process of **A** to **Ats**

Items	TS	P_1C_1 (Å)	P_1O_2 (Å)	C_1O_1 (Å)	O_1H_1 (Å)	O_2H_1 (Å)	α	O_1M (Å)	O_3M (Å)	[f + M]$^{+a}$
[**3a** + Na]$^+$	20.8	2.606	1.645	1.252	2.038	0.978	138.8	2.226	2.193	1.8%
[**3b** + Na]$^+$	21.6	2.578	1.643	1.257	2.028	0.979	137.9	2.211	2.194	1.6%
[**3c** + Na]$^+$	22.3	2.700	1.652	1.249	2.108	0.977	138.8	2.219	2.196	0.9%
[**3c** + Na]$^{+b}$	22.4	2.700	1.652	1.249	2.108	0.977	138.8	2.219	2.196	0.9%
[**3d** + Na]$^+$	22.8	2.253	1.616	1.279	1.885	0.990	132.6	2.251	2.254	1.6%
[**3e** + Na]$^+$	22.8	2.919	1.664	1.239	2.194	0.974	140.7	2.237	2.195	1.2%
[**3f** + Na]$^+$	11.3	2.696	1.668	1.249	1.884	0.981	134.9	2.193	2.138	68.0%
[**3f** + Li]$^+$	9.5	2.440	1.675	1.266	2.037	0.981	114.7	1.838	1.795	9.3%
[**3f** + K]$^+$	15.2	3.046	1.669	1.235	1.962	0.976	152.1	2.633	2.595	92.6%

[a]The ratio of the intensity of the [f + M]$^+$ ions to the sum of the intensities of all the products.
[b]Deuteration of [**3c** + Na]$^+$.

Rapid Communications in Mass Spectrometry

all the compounds in Table 3. The results indicate that a steric effect controls the activation energy of the transition state, which is in good accord with experimental data (see the TS column and $[f + M]^+$ column in Table 3 from entry $[\mathbf{3a} + Na]^+$ to $[\mathbf{3f} + Na]^+$). The $[\mathbf{3f} + Na]^+$ compounds have the lowest transition state energy (11.3 kcal mol^{-1}), about 10 kcal mol^{-1} lower than for other compounds. Furthermore, the bond lengths of O_1Na (2.193 Å) and O_3Na (2.138 Å) in the $[\mathbf{3f} + Na]^+$ transition state are about 0.2–0.3 Å shorter than others and this species also has the shortest O_1H_1 bond length (1.884 Å). Evidently, the transition state of $[\mathbf{3f} + Na]^+$ is more product-like. On the other hand, the sodium ion might have a stronger coordination interaction with the carbonyl group of $[\mathbf{3f} + Na]^+$ to stabilize the rearrangement product **3f[f]** (see Scheme 3 for the structure of **3f[f]**), which also pushes the H1 proton much closer to O2 of the phosphoryl group. This process could reduce the activation energy significantly (about 10 kcal mol^{-1}) and hence produce a greater abundance of rearrangement ions. The order of activation energy {$[\mathbf{3f} + Na]^+$ (11.3 kcal mol^{-1}) < $[\mathbf{3a} + Na]^+$ (20.8 kcal mol^{-1}) < $[\mathbf{3b} + Na]^+$ (21.6 kcal mol^{-1}) < $[\mathbf{3c} + Na]^+$ (22.3 kcal mol^{-1})} is exactly in accord with the experimental results {$[\mathbf{3f} + Na]^+$ (68%) < $[\mathbf{3a} + Na]^+$ (1.8%) < $[\mathbf{3b} + Na]^+$ (1.6%) < $[\mathbf{3c} + Na]^+$ (0.9%)}, which reveals that this steric effect regulation process is kinetically controlled, but not thermodynamically.

Because the rearrangement behavior of **3f** is assisted by a sodium ion, the role of different ions such as H^+, Li^+, Na^+, K^+ was studied by ESI-MS^n. It was found that sodium and potassium ion adducts have a stronger ability to rearrange. By contrast, there are no rearrangement ions of product $[\mathbf{3f} + H]^+$ ($[f + H]^+ = 0$) in the absence of metal ion assistance. The likely reason is that a proton has weak coordination ability and so leads to a totally different fragmentation pattern compared with our proposed five-membered ring proton migration. It is thus clear that this rearrangement only occurs in the presence of metal ions. We therefore modelled the process to investigate how metal ions influence the rearrangement process. The results show that all the MS rearrangement reactions of species **3f** occur easily with a low energy of activation. The order of activation energy is $[\mathbf{3f} + Li]^+$ (9.5 kcal mol^{-1}) < $[\mathbf{3f} + Na]^+$ (11.3 kcal mol^{-1}) < $[\mathbf{3f} + K]^+$ (15.2 kcal mol^{-1}). It is surprising that this sequence is the opposite of the experimental results: $[\mathbf{3f} + Li]^+$(9.3%) < $[\mathbf{3f} + Na]^+$ (68.0%) < $[\mathbf{3f} + K]^+$ (92.6%). It could be that this ion-induced five-membered ring transition state is not the rate-determining step in the metal-assisted rearrangement of compound **3f**. Indeed, this process could be controlled thermodynamically.

CONCLUSIONS

We have investigated the fragmentation behavior of a series of synthetic phosphonate esters. The MS/MS fragmentation pathways for these sodium salt species are described and rationalized. Assisted by sodium ion coordination, alkyl groups are easily lost from phosphonates by C–O bond cleavage. When no alkoxy group is connected directly to the phosphorus atom, as for compound **3f**, an intermolecular proton transfer process can occur. Isotope deuterium/hydrogen exchange experiments combined with high-resolution mass spectra support that this fragmentation process involves a five-membered ring concerted transition state $[\mathbf{3f} + Na]^+$–**Ats** (see Scheme 3). The activation energy calculated by B3LYP/6-31 G* is 11.3 kcal mol^{-1}, so this fragmentation process is readily achievable by excitation at the high energies afforded in the ion trap of a mass spectrometer. Whereas the overall reaction is endothermic at about 13.2 kcal mol^{-1}, this cleavage process can be considered as the reverse of the synthetic pathway used for all of these compounds. Finally, from a study of fragmentation for different metal cations (H^+, Li^+, Na^+, K^+), we see that the adduct of **3f** with Na^+ or K^+ gives fragment $[f + M]^+$ with high relative intensity.

SUPPORTING INFORMATION

Additional supporting information may be found in the online version of this article.

Acknowledgements

We would like to acknowledge financial support from the Major Program of National Natural Science Foundation of China (No. 20732004) and the National Natural Science Foundation of China (Nos. 20805037, 20972130 and 21075103). We thank Prof. G. M. Blackburn for useful discussions and suggestions.

REFERENCES

[1] M. Horiguchi, M. Kandatsu. Isolation of 2-aminoethane phosphonic acid from rumen protozoa. *Nature* **1959**, *184* (Suppl 12), 901.
[2] S. C. Fields. Synthesis of natural products containing a C–P bond. *Tetrahedron* **1999**, *55*, 12237.
[3] O. I. Kolodiazhnyi. Asymmetric synthesis of hydroxyphosphonates. *Tetrahedron-Asymmetry* **2005**, *16*, 3295.
[4] P. P. Giannousis, P. A. Bartlett. Phosphorus amino acid analogs as inhibitors of leucine aminopeptidase. *J. Med. Chem.* **1987**, *30*, 1603.
[5] D. V. Patel, K. Rielly-Gauvin, D. E. Ryono, C. A. Free, W. L. Rogers, S. A. Smith, J. M. DeForrest, R. S. Oehl, E. W. Petrillo. alpha-Hydroxy phosphinyl-based inhibitors of human renin. *J. Med. Chem.* **1995**, *38*, 4557.
[6] X.-L. Chen, L.-B. Qu, T. Zhang, H.-X. Liu, F. Yu, Y. Yu, X. Liao, Y.-F. Zhao. The nature of phosphorylated chrysin – protein interactions involved in noncovalent complex formation by electrospray ionization mass spectroscopy. *Anal. Chem.* **2003**, *76*, 211.
[7] M. Yamashita, J. B. Fenn, Negative ion production with the electrospray ion source. *J. Phys. Chem.* **1984**, *88*, 4671.
[8] M. D. Bauer, Y. Sun, F. Wang. Sequencing of gel-isolated proteins using microblotter capillary liquid chromatography-electrospray mass spectrometry. *J. Protein Chem.* **1999**, *18*, 337.
[9] H. Wu, H. Aboleneen. Improved oligonucleotide sequencing by alkaline phosphatase and exonuclease digestions with mass spectrometry. *Anal. Biochem.* **2001**, *290*, 347.
[10] X. Z. Qin, Y. H. Wu, Z. Zhao, X. Chen. Collision-induced dissociation of protonated MK-0991: Novel ring opening of a cyclic hexapeptide in the gas phase. *J. Mass Spectrom.* **1999**, *34*, 733.
[11] X. Z. Qin. Tandem mass spectrum of a farnesyl transferase inhibitor - gas-phase rearrangements involving imidazole. *J. Mass Spectrom.* **2001**, *36*, 911.

[12] M. J. Frisch, G. W. Trucks, H. B. Schlegel, G. E. Scuseria, M. A. Robb, J. R. Cheeseman, J. A. Montgomery, Jr., T. Vreven, K. N. Kudin, J. C. Burant, J. M. Millam, S. S. Iyengar, J. Tomasi, V. Barone, B. Mennucci, M. Cossi, G. Scalmani, N. Rega, G. A. Petersson, H. Nakatsuji, M. Hada, M. Ehara, K. Toyota, R. Fukuda, J. Hasegawa, M. Ishida, T. Nakajima, Y. Honda, O. Kitao, H. Nakai, M. Klene, X. Li, J. E. Knox, H. P. Hratchian, J. B. Cross, V. Bakken, C. Adamo, J. Jaramillo, R. Gomperts, R. E. Stratmann, O. Yazyev, A. J. Austin, R. Cammi, C. Pomelli, J. W. Ochterski, P. Y. Ayala, K. Morokuma, G. A. Voth, P. Salvador, J. J. Dannenberg, V. G. Zakrzewski, S. Dapprich, A. D. Daniels, M. C. Strain, O. Farkas, D. K. Malick, A. D. Rabuck, K. Raghavachari, J. B. Foresman, J. V. Ortiz, Q. Cui, A. G. Baboul, S. Clifford, J. Cioslowski, B. B. Stefanov, G. Liu, A. Liashenko, P. Piskorz, I. Komaromi, R. L. Martin, D. J. Fox, T. Keith, M. A. Al-Laham, C. Y. Peng, A. Nanayakkara, M. Challacombe, P. M. W. Gill, B. Johnson, W. Chen, M. W. Wong, C. Gonzalez, J. A. Pople. *Gaussian 03, Revision C.02*, Gaussian, Inc., Wallingford, CT, **2004**.

[13] A. D. Becke. Density-functional thermochemistry. III. The role of exact exchange. *J. Chem. Phys.* **1993**, *98*, 5648.

[14] C. Lee, W. Yang, R. G. Parr. Development of the Colle-Salvetti correlation-energy formula into a functional of the electron density. *Phys. Rev. B* **1988**, *37*, 785.

[15] P. C. Hariharan, J. A. Pople. The effect of d-functions on molecular orbital energies for hydrocarbons. *Chem. Phys. Lett.* **1972**, *16*, 217.

[16] M. M. Francl, W. J. Pietro, W. J. Hehre, J. S. Binkley, M. S. Gordon, J. D. DeFrees, J. A. Pople. Self-consistent molecular orbital methods. XXIII. A polarization-type basis set for second-row elements. *J. Chem. Phys.* **1982**, *77*, 3654.

[17] A. N. Pudovik, I. V. Konovalova. Addition reactions of esters of phosphorus(III) acids with unsaturated systems. *Synthesis* **1979**, *81*.

[18] J. C. Traeger, A. Luna, J. C. Tortajada, T. H. Morton. Regio- and stereochemistry of alkene expulsion from ionized sec-alkyl phenyl ethers. *J. Phys. Chem. A* **1999**, *103*, 2348.

[19] C. Hudson, D. McAdoo. 1,2-Eliminations from $(CH_3)_2NH^+CH_2CH_3$ and $(CH_3)^2NH^{2+}$: Guided dissociations. *J. Am. Soc. Mass Spectrom.* **2008**, *19*, 1491.

[20] C. Wolf, C. N. Villalobos, P. G. Cummings, S. Kennedy-Gabb, M. A. Olsen, G. Trescher. Elucidation of the presence and location of t-Boc protecting groups in amines and dipeptides using on-column H/D exchange HPLC/ESI/MS. *J. Am. Soc. Mass Spectrom.* **2005**, *16*, 553.

[21] S. Cao, J. Zhang, J. Xu, X. Liao, Y. Zhao. Electrospray tandem mass spectrometric studies of all twenty N-phosphoryl amino acids. *Rapid Commun. Mass Spectrom.* **2003**, *17*, 2237.

[22] Y. W. Yin, Y. Ma, Y. F. Zhao, B. Xin, G. H. Wang. Negative-ion fast atom bombardment mass spectrometry of N-phosphoamino acids. *Org. Mass Spectrom.* **1994**, *29*, 201.

[23] Y. F. Zhao, D. Q. Zhang, C. B. Xue, J. N. Zeng, G. J. Ji. Novel fragmentation of *N*-diisopropyloxyphosphoryl dipeptides and tripeptides by fast atom bombardment mass spectrometry. *Org. Mass Spectrom.* **1991**, *26*, 510.

[24] H. Fang, M. J. Fang, C. J. Zhu, L. N. Liu, Y. F. Zhao. Study on [(4-substituted benzoylamino)phenylmethyl]phosphonic acid diisopropyl esters under electrospray ionization tandem mass spectrometric conditions. *Rapid Commun. Mass Spectrom.* **2007**, *21*, 3629.

